International Journal on Interactive Design and Manufacturing (IJIDeM)

A Bio-inspired Grasp Optimization Algorithm for an Anthropomorphic Robotic Hand

--Manuscript Draft--

Manuscript Number:	
Full Title:	A Bio-inspired Grasp Optimization Algorithm for an Anthropomorphic Robotic Hand
Article Type:	Original Paper
Corresponding Author:	Francesca Cordella Università di Napoli Federico II Naples, ITALY
Corresponding Author Secondary Information:	
Corresponding Author's Institution:	Università di Napoli Federico II
Corresponding Author's Secondary Institution:	
First Author:	Francesca Cordella
First Author Secondary Information:	
Order of Authors:	Francesca Cordella
	Loredana Zollo
	Eugenio Guglielmelli
	Bruno Siciliano
Order of Authors Secondary Information:	
Abstract:	A fundamental requirement for assistive robots is to guarantee a safe and human-like way to perform their tasks. In particular, the ability to realize smooth movements and obtain a stable grasp is of primary importance. In this perspective, this paper aims at studying human grasping and developing a bio-inspired method for power-grip posture prediction and finger trajectory planning for a robotic hand. The developed method is based on neuroscientific assumptions and experimental evidence coming from the observation of the human behavior during power grip. It is based on the minimization of a suitably defined function to identify the optimal grasp configuration and the choice of a logarithmic spiral trajectory for moving the fingers. The behavior of ten different subjects during the grasping action has been analyzed with the CyberGlove motion capture data glove. A common thumb posture has been observed and has been introduced in the grasping algorithm. The algorithm performance has been tested on an anthropomorphic robotic hand by means of simulation trials. The results demonstrate the effectiveness of the approach and pave the way for the implementation on a real robotic hand.

*Title Page

A Bio-inspired Grasp Optimization Algorithm for an Anthropomorphic Robotic Hand

F. Cordella[1], L. Zollo[2], E. Guglielmelli[3] , B. Siciliano[4]

(1,4): *PRISMA Lab, Dipartimento di Informatica e Sistemistica, Università di Napoli Federico II, via Claudio 21, 80125 Napoli, Italy*

E-mail: {francesca.cordella, bruno.siciliano}@unina.it

(2,3): *Laboratory of Biomedical Robotics and Biomicrosystems,*

Università Campus Bio-Medico, via Alvaro del Portillo 21, 00128 Roma,Italy

E-mail: {l.zollo, e.guglielmelli}@unicampus.it

Noname manuscript No.
(will be inserted by the editor)

A Bio-inspired Grasp Optimization Algorithm for an Anthropomorphic Robotic Hand

the date of receipt and acceptance should be inserted later

Abstract

A fundamental requirement for assistive robots is to guarantee a safe and human-like way to perform their tasks. In particular, the ability to realize smooth movements and obtain a stable grasp is of primary importance. In this perspective, this paper aims at studying human grasping and developing a bio-inspired method for power-grip posture prediction and finger trajectory planning for a robotic hand. The developed method is based on neuroscientific assumptions and experimental evidence coming from the observation of the human behavior during power grip. It is based on the minimization of a suitably defined function to identify the optimal grasp configuration and the choice of a logarithmic spiral trajectory for moving the fingers. The behavior of ten different subjects during the grasping action has been analyzed with the CyberGlove motion capture data glove. A common thumb posture has been observed and has been introduced in the grasping algorithm. The algorithm performance has been tested on an anthropomorphic robotic hand by means of simulation trials. The results demonstrate the effectiveness of the approach and pave the way for the implementation on a real robotic hand.

Keywords grasping · bio-inspired · preshaping · robotic hand · Cyberglove

1 Introduction

Since the robots utilized in the field of assistive robotics have to be designed for aiding humans in their daily living tasks, a safe human-robot interaction is an essential requirement. With special reference to the upper limb, it should be guaranteed that the robotic hand is able to realize a successful grasp by approaching the object with an optimal configuration. In other words, grasping has to be stable and thus requires an optimal control of both hand posture and motion.

Being the human hand a wonderful example of a highly dexterous system, due to its complex mechanical structure and versatility in multiple activities, a bio-inspired approach has been pursued in this work. Consequently, a thoroughly study of the human hand, as regards the anatomy as well as the hand behavior during grasping, has been carried out.

The performed analysis has led to useful information for developing human-like grasping algorithms and improving knowledge about hand kinematics. This could potentially provides new insights into the design of anthropomorphic robotic hands endowed with high dexterity and innovative rehabilitation devices that guarantee a safe and natural human-robot interaction.

The pursued approach consists of searching the better grasping configuration enabling a stable grasp, in order to reduce complexity of the control. During the pre-shaping phase, in fact, while approaching the object, the hand assumes the most suitable configuration for seizing [1], [2], [3] on the basis of the physical characteristics of the object to be grasped, such as shape and weight. During this phase, the contact points between the fingers and the object allowing a stable grasp are also determined, and the trajectory to be followed by the fingers is planned in order to grasp the object in the determined points. A stable grasp is therefore guaranteed by finding the most appropriate hand configuration.

In order to identify the most common hand configurations, some grasp taxonomies have been introduced

Address(es) of author(s) should be given

in the literature. By considering only the characteristics of the object the hand interacts with, Schlesinger [4] divided the human hand grasping configurations into six different types of prehension. However, in this classification the task to be performed is not considered, whilst actually the choice of the grasping modality is mainly dictated by the task to be accomplished. In [5], [6], [7], [8], [9], [10] some taxonomies are proposed according to the task. In particular, two principal classes of grasps are distinguishable: power grasp, in which the whole hand is involved, and precision grasp, where only fingers are involved.

This paper is focused on the analysis of the power grasp, since it is one of the five types of grasps mostly used in daily life [11]. Further, among power grasps, attention has mainly been focused on diagonal volar grasp, the type of cylindrical power grasp, discussed in [12], where the thumb is adducted lying along the longest axis of the object (Fig. 1). In this case, in [12] the hand configuration is predicted by modelling the finger and object surface with ellipsoids and by applying an optimization algorithm for determining the contact points between ellipsoids. The principal drawback of this approach is that the MetaCarpo-Phalangeal (MCP) joint adduction/abduction angle is assumed to be equal to zero and that the thumb adduction/abduction angles are not estimated. The thumb behavior is neglected also in [13], where a criterion for determining long fingers optimal configuration for grasping cylindrical objects with a diagonal volar grasp is presented.

Fig. 1 Diagonal volar grasp.

The majority of research studies about the identification of an optimal grasp configuration are based on the determination of the contact points by considering the contact forces [14], [15]. On the contrary, this work starts proposing a kinematic approach —to be potentially integrated with a further analysis on hand dynamics— since it is aimed at preliminarily assessing the role of the kinematic structure of the hand and of the fingers in the design of an assistive device devoted to interact with humans. To this purpose, the thumb behavior is here also introduced by using the data obtained with a data glove for motion analysis. The aim of the preshaping optimization algorithm presented in this paper is to find an optimal hand configuration for grasping cylindrical objects with a diagonal volar grasp. The proposed approach has a reduced computation cost and is based on the minimization of a suitable objective function and on the introduction of the constraints obtained from the analysis of the human grasping action.

Once the hand configuration for an optimal grasp has been defined, it is necessary to establish the trajectory that the fingers should follow in order to get the final grasp configuration. In order to overcome this problem, over the years the mechanical structure of robotic hands has been considered along with algorithms for improving grasping naturalness. For instance, in [16] under-actuated prosthetic hands that try to reproduce the gradual moulding of the hand on the object contour by automatically adapting themselves to the object shape are introduced. In [17] the minimum jerk approach is fitted to a prosthetic finger. The main drawback is that the approach is suited only for straight movements in the xy-plane, while the fingers trajectory of the human hand is curved. Two optimization-based models are proposed in [18]. In the former approach, the function to be minimized is analogous to the kinetic energy. It implies constant velocity and acceleration, which are in contrast with the observed boundary conditions in natural point-to-point movements of zero joint velocity and acceleration at the start and end of the movement. The latter approach, based on minimum torque-change cost function, has the drawback that the curvature of the finger path is opposite to that observed in experiments on human beings. In a prosthetic hand driven by electromyographic signals (EMG), for example, once the command given by the patient has been interpreted, the prosthetic hand has to move autonomously following a suitable trajectory. In this paper, taking inspiration from [19], the fingertip movement is modelled with a logarithmic spiral.

The paper is organized as follows: in Section 2 the hand motion analysis, performed with the CyberGlove, is described and the results are analyzed; in Section 3 the preshaping and the finger trajectory planning algorithms are described; in Section 4 the validation of the algorithm on a robotic hand model is presented. Finally, conclusions and future developments are presented in Section 5.

2 Analysis of human grasping action

2.1 Human hand kinematic model

In order to model the kinematic structure of the human hand, each finger can be modelled by a kinematic chain and the wrist can be considered as the origin of the reference frame. The type of joint utilized in the model is chosen on the basis of the degrees of freedom (DOFs) associated with it. It is known in [20] that the MCP joint has 2 DOFs; therefore, it is convenient to model it as an ellipsoidal joint that enables flexion/extension as well as limited lateral deviation. Since Proximal Intra-Phalangeal (PIP) and Distal Intra-Phalangeal (DIP) joints have 1 DOF each, they can be modelled with hinge joints enabling movements only in one direction. The thumb MCP joint is a saddle joint that gives the thumb the ability to cross over the palm of the hand (Fig. 2).

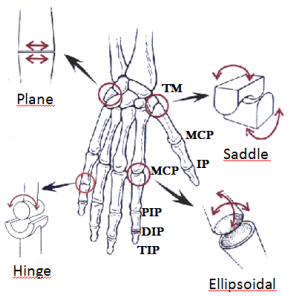

Fig. 2 Human hand joints.

In order to find a valid kinematic model, different kinematic models presented in the literature [21], [22], [23], [24], [25] have been analyzed. For simplifying the hand model, the most commonly used hand motion constraints [26], [27] have been considered. They regard the range of motion of the finger joints due to the hand structure, the abduction of the middle finger (an approximation of 0 degrees for this angle is commonly adopted), and the correlation among the PIP and DIP joints of the long fingers ($\theta_{DIP} = \frac{2}{3}\theta_{PIP}$).

From the above considerations it has been decided to represent the kinematic chain of the human fingers as shown in Fig. 3, where (for the sake of clarity) only the thumb and the index finger kinematic chain are shown. Middle, ring and little fingers have the same kinematic chain of the index finger. The modelling of the hand joints has been made by merging information about the joint axis of rotation taken from the literature [21], [22], [28] and the joint angle values given by the Cyberglove (Virtual Technologies, Palo Alto, CA) sensors used in the analysis of human hand motion in Section 2.2. The MCP and Inter-Phalangeal (IP) joints of the thumb and the PIP and DIP joints of the index have been modelled as a hinge joint with 1 DOF. The TrapezioMetacarpal (TM) joint of the thumb and the MCP joint of the index finger have been modelled as ellipsoidal joints with perpendicular rotational axis and 2 DOFs. The center of the root coordinate system is the center of the wrist (Fig. 3). In the shown kinematic model, the flexion/extension axis of the TM joint has been considered perpendicular to the adduction/abduction axis. Although in the human hand these two axes are inclined of about 73^o, it has been chosen to maintain them orthogonal for computational reasons and for better matching the positions of the CyberGlove sensors. In this kinematic model, it has been supposed that the adduction/abduction movement of the thumb is due essentially to the TM joint, and thus it has been supposed that the MCP joint has only 1 DOF.

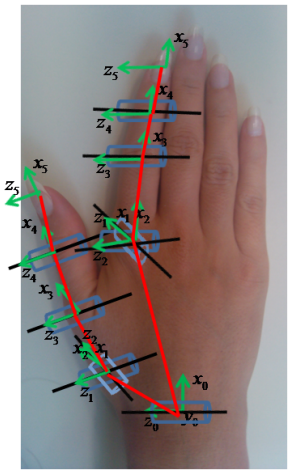

Fig. 3 Human hand kinematic model. The middle, ring and little fingers have the same kinematic chain of the index finger.

The Denavit-Hartenberg parameters for the index finger and for the thumb are shown in Tabs. 1 and 2, respectively. The introduced kinematic model has been used in the following section for analyzing the data acquired with the CyberGlove.

Table 1 Denavit-Hartenberg parameters of the index finger.

Link #	d	θ	$a\,[m]$	α
1	$d_{1_{\text{index}}}$	θ_1	Mc	$-\frac{\pi}{2}$
2	0	θ_2	0	$\frac{\pi}{2}$
3	0	θ_3	P_{index}	0
4	0	θ_4	M_{index}	0
5	0	θ_5	D_{index}	0

Table 2 Denavit-Hartenberg parameters of the thumb

Link #	d	θ	$a\,[m]$	α
1	$d_{1_{\text{index}}}$	θ_1	Tm	$-\frac{\pi}{2}$
2	$d_{2_{\text{index}}}$	θ_2	0	$\frac{\pi}{2}$
3	0	θ_3	P_{thumb}	0
4	0	θ_4	M_{thumb}	0
5	0	θ_5	D_{thumb}	0

2.2 Experiments on human subjects with CyberGlove

The CyberGlove$^{\text{TM}}$ [29] is a motion capture data glove fully instrumented with 22 resistive bend sensors that measure the five finger joint angles. In Fig. 4, the positions of the Cyberglove sensors are indicated with yellow circles. The data glove uses resistive bend-

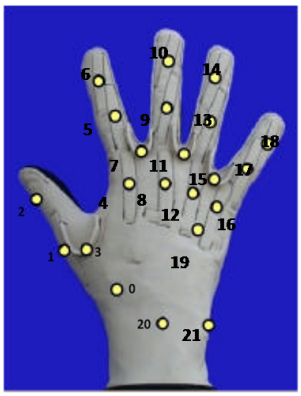

Fig. 4 CyberGlove with joint sensor locations outlined by yellow circles.

sensing technology to accurately transform hand and finger motions into real-time digital joint-angle data. The sampling frequency used by the CyberGlove is 30 Hz.

The grasping experiments involved ten human subjects, 22.4 years old on average (with 1.5 Standard Deviation), all men and right handed. Subjects have been asked to wear the 22 sensorized CyberGlove with the right hand, and to grasp a cylindrical object with the diagonal volar grasp introduced before.

The participants have been seated in front of a table on which the object has been located in a-priori known position. The hand starting position and initial posture have been the same for all the participants (Fig. 5). The object has been positioned at a distance of 53 cm from the sensor on the wrist and the starting hand configuration has consisted of the four fingers fully extended and the thumb adducted. The hand joint angles have been recorded in this starting position and in the position in which the hand is completely closed around the object. Before starting the test, the lengths of each

Fig. 5 Starting position of the subjects with respect to the table on which the object has been located.

finger segment (distal, medial, proximal phalanx and metacarpal phalanx of the thumb) of each subject have been measured with a caliber. Lengths have been measured as the distances between the two extreme bones of the link. These data have been used for constructing the hand forward kinematics.

Every subject have been asked to grasp the object, without lifting it, fifteen times, the first five of which have been useful for learning the grasping action, therefore only the data about the last ten trials have been acquired. The data acquisition of each trial has been started with a voice command. After grasping the object, the subject has remained in this grasping position till an auditory signal announced the acquisition end.

Particular attention has been paid to the thumb behavior during grasping through a specific parameter extracted from the position values supplied by the sensors placed on the thumb and the index finger, i.e. the opening angle. It is computed as the angle between the link connecting the MCP joint of the thumb and the wrist, and the link connecting the MCP joint of the index finger and the wrist. This parameter is useful for having information about the position of the thumb during grasping and can be evaluated once a kinematic model of the hand has been defined. To this purpose, the hand kinematic model introduced in Section 2.1 has been used for determining the hand joint positions needed for computing the opening angle.

In Tab. 3 the mean and standard deviation of the hand opening angle for each subject during the 10 trials are reported. From the table it is possible to note a quite invariant behavior on each subject and among subjects as regards the diagonal volar grasp. This consideration has led us to formulate a general rule about the thumb configuration during this type of grasp, which can be used to extend to five fingers the grasping algorithm we presented in [30]. This algorithm will be briefly explained in Sect. 3.1.

Table 3 Mean and standard deviation of hand opening angle in diagonal volar grasp.

Subject #	Mean	SDV
1	48.63^o	0.77^o
2	49.56^o	1.33^o
3	50.40^o	1.51^o
4	45.87^o	1.45^o
5	45.42^o	1.21^o
6	51.46^o	0.65^o
7	52.57^o	1.18^o
8	50.29^o	0.68^o
9	45.83^o	0.82^o
10	49.75^o	0.93^o

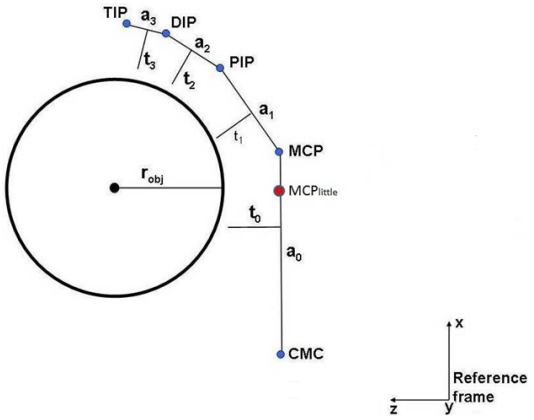

Fig. 6 Working scenario. The little MCP joint position is outlined in red.

3 Grasping algorithm

3.1 Optimization algorithm

The grasping algorithm presented in [30] resorts to biomechanics results regarding the behavior of the four long fingers (index, middle, ring and little) during a diagonal volar grasp [13]. According to these results, when a human subject grasps a cylinder with a diagonal volar power grasp, the best configuration is the one that minimizes the distances between hand joints and object surface. Starting from this assumption, we implemented an algorithm that minimizes an objective function given by the sum of the joint distances from the object surface. The expression of the objective function is the following

$$f = \sum_{i=1}^{4} \sum_{j=1}^{3} dist_j^i(x, \alpha), \tag{1}$$

where: i is the finger index, ranging from 1 (the index finger) to 4 (the little finger); j is the joint index, ranging from 1 (the MCP joint) to 3 (the DIP joint); $dist_j^i$ is the distance of the joint j of the i-th finger from the centre of rotation (COR) and $dist_j^i$ is a function of the parameters x and α which are, respectively, the x-coordinate of the wrist joint (here called CarpoMetaCarpal, CMC, joint) and the inclination angle of the object rotation axis with respect to y-axis of a reference frame centred in the hand CMC joint. It has been supposed that the hand has a starting position close to the object, corresponding to a reaching phase almost finished (Fig. 6). The position of the object and of the hand joints (MCP, PIP and DIP) are computed with respect to this reference system. The object is located in a given position on the xz plane: namely, the object is at a distance of 9.5 cm on x-axis, along which the hand moves longitudinally, and of 10 cm on z-axis, along which the hand moves laterally. The x-coordinate of the CMC joint that guarantees an optimal grasping position of the hand is obtained by minimizing the objective function (1). In order to guarantee the stability of the grasp, it is assumed that the y-coordinate of CMC joint coincides with that of the object centre of rotation (COR). This assumption is grounded on studies on human beings that have demonstrated as the position of the contact points between the hand and the object depends on the location of the object centre of mass (CM) [31]. Thus, in our case, the vertical location of the MCP joint of the middle finger is in the middle of the object. The same consideration can be applied to CMC joint, since the two joints are aligned; accordingly, the CMC z-coordinate is set equal to that of MCP joint.

Once determined the CMC joint position, the algorithm provides a new hand configuration, expressed in the reference frame, and corresponding to the optimal grasp of a specific object able to ensure grasp stability. The hand joint positions have been obtained by minimizing the following distances

$$dist_{MCP}^i = \sqrt{(x_{MCP_i} - x_{obj})^2 + (r_{obj} + t_0)^2} \tag{2}$$

$$dist_{PIP}^i = \sqrt{(a_1 - \sqrt{(r_{obj} + dist_{MCP}^i)^2 - (r_{obj} + t_1)^2})^2 + (r_{obj} + t_1)^2} \tag{3}$$

$$dist_{DIP}^i = \sqrt{(a_2 - \sqrt{(r_{obj} + dist_{PIP}^i)^2 - (r_{obj} + t_2)^2})^2 + (r_{obj} + t_2)^2} \tag{4}$$

where a_i is the finger length, t_i is the finger thickness, r_obj is the object radius,

$$x_{MCP_i} = x + (x_{MCP_i}^{\text{start}} - x_{MCP_4}^{\text{start}}) + (y_{MCP_i}^{\text{start}} - y_{MCP_4}^{\text{start}}) * tan\alpha \tag{5}$$

is the z-coordinate of the MCP joint of the i-th finger in the optimal configuration. Its value depends on the z-coordinate of the initial configuration (i.e. $x_{MCP_i}^{\text{start}}$). The x coordinate of the little MCP joint is a reference point of the optimization algorithm.

Note that what previously explained is valid when fingers are orthogonal to the object rotation axis. This

is an ideal assumption that has preliminarily been done in order to simplify the problem. In order to adapt the results to the real case where the fingers are inclined with respect to the object rotation axis, it is necessary to work on the projection plane. To be more specific, in the human hand, MCP joints are inclined of a certain angle with respect to wrist CMC joint, and the fingers (i.e. the link between the MCP joints and the TIP) form a certain angle with respect to the corresponding MCP joints. It is then necessary to modify expressions (1)–(4) for considering those inclinations. This is achieved by replacing parameters related to the link lengths in (1)–(4), i.e. a_i with their projections in the plane perpendicular to the object rotation axis. In fact, Equations (1)–(4) are still valid if they are used in the plane perpendicular to the cylindrical object rotation axis.

The link length projection value l_i is determined in the perpendicular plane using the following expression

$$\| l_i \| = \sqrt{(\| a_i \|^2 - \| a_i \bullet (n_p \times n_o) \|^2) \bullet (n_p \bullet n_o)^2 + \| a_i \bullet (n_p \times n_o) \|^2} \quad (6)$$

where l_i is the projection of link length a_i, while $n_p \times n_o$ and $n_p \bullet n_o$ are, respectively, the cross product and the dot product between the unit normal vector n_p of the plane perpendicular to the object rotation axis and the unit normal vector n_o of the oblique plane where the fingers lie. Therefore, Equations (1)–(4), modified with these new length values, are the new set of equations to apply in the case of inclined fingers.

By using the so obtained distance values, the joint angles in the projection plane are determined. The results are brought back to the original plane, i.e. the inclined plane with respect to the cylinder rotation axis. Joint Cartesian coordinates in the original plane are given by the intersection of that plane with the straight-line perpendicular to the original plane and passing through the joint in the projection plane.

Joint angles are determined by means of inverse kinematics, starting from joint Cartesian coordinates. The constraint on the DIP and PIP flexion angles, according to which $\theta_{DIP} = \frac{2}{3}\theta_{PIP}$, has been used for coupling the two joints.

In addition to the illustrated results, detailed in [30], the thumb behavior has been introduced in the model. This was possible on the basis of the results exposed in Sect. 2.2, showing that the opening angle is quite invariant from subject to subject when a diagonal volar grasp is performed. In particular, thumb configuration in the space was established resorting to the following considerations:

- The knowledge of the opening angle, together with the minimization of the distances from the thumb joints and the object surface by means of (2)–(5), implies the possibility of determining MCP joint position with respect to CMC joint.
- The other thumb joints have the same y-coordinate of MCP thumb joint. In order to determine the thumb TIP optimal position, the IP flexion angle measured with the CyberGlove is considered. It has been observed that its value is similar among the ten subject and is around 18^o.

3.2 Trajectory planning algorithm

Once the optimal hand joint positions have been determined, it is necessary to move the fingers from the initial configuration to the final one given by the preshaping optimization algorithm, by following a reference trajectory. On the basis of studies on human beings [19], it is possible to say that the fingertip motion during grasping follows a logarithmic spiral trajectory. In the Cartesian space, the time-varying coordinates of the TIPs can be expressed as

$$\begin{cases} x(t) = r\cos\theta(t) \\ y(t) = r\sin\theta(t). \end{cases} \quad (7)$$

They correspond to a logarithmic spiral in polar coordinates

$$r = ae^{b\theta} \quad (8)$$

where r is the spiral radius, a is a coefficient that rotates the spiral, b is a coefficient that controls the spiral pitch and twins direction, and θ is the angle between the radius and the z-axis of the reference frame centred in the MCP joint. It is evident that the radius of the spiral depends on the spiral inclination angle θ that fingers sweep. Equations (7)–(8) allow determining the points the fingertips will pass through when moving from the initial position (open hand close to the object) to the final position computed by the minimization algorithm (Fig. 7).

The joint angles corresponding to the TIP positions during grasping are obtained through the inverse kinematics. A proportional-derivative control in the joint space is used to make the hand track the reference trajectory of (8).

A schematic representation of how the two algorithms work together is shown in Fig. 7: starting from information about initial joint angles, the optimization algorithm gives the joint positions that the hand should assume at the end of the grasping action for a stable grasp. The algorithm returns also CMC optimal position near the object. After the reaching phase, initial finger joint angles and optimal finger joint angles are given in input at the planning algorithm producing the trajectory that the fingers will follow for a natural grasping action.

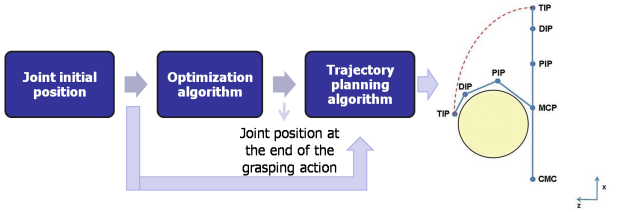

Fig. 7 Finger position at the beginning and at the end of the trajectory.

4 Simulation results

In order to test the effectiveness of the approach simulation trials have been carried out. A virtual robotic hand has been modelled with the same mechanical characteristics of a real human hand (Fig. 3). In Tab. 4 the geometric parameters of the hand and of the cylindrical object to be grasped are reported. The Matlab function $fminsearch(f, [initialcondition])$ has been used for minimizing the objective function f starting from the conditions specified by $[initialcondition]$. The result of the minimization is the x-coordinate of CMC joint that guarantees a stable grasp. The CMC optimal position is completely given by adding its y and z-coordinates determined as previously explained. Adapting (2)–(5) to the case of inclined fingers and considering the hand parameters given in Tab. 4, the coordinates of MCP, PIP and DIP joints are determined. Information about the thumb is also introduced as explained in Sect. 3.1.

Table 4 Geometric parameters of the simulated hand and object.

Symbol	Link name	value$[m]$
a_0	$CMC - MCP$ link length	0.075
a_1	Proximal link length	0.045
a_2	Medial link length	0.025
a_3	Distal link length	0.023
t_0	Palm thickness	0.025
t_1	Proximal link thickness	0.010
t_2	Medial link thickness	0.0075
t_3	Distal link thickness	0.0025
r_{obj}	Cylindrical object radius	0.0255

Matlab simulation results are reported in Fig. 8. Looking at the stick figure, the finger thickness should be considered thus causing the contact with the object; the represented points are finger joints and the sticks represent the link length (without thickness). The joints of each finger are outlined with different colors: the red dot is the CMC joint, the green dots are the MCP, PIP and DIP joints of the index finger, blue dots are MCP, PIP and DIP joints of the middle finger, magenta dots are MCP, PIP and DIP joints of the ring finger and black dots are the MCP, PIP and DIP joints of the little finger. As previously said, with respect to the reference frame centred in the CMC joint of the hand in the starting configuration, the x and y-coordinates of the object center are 9.5 cm and 10 cm, respectively. The object height is 15 cm, therefore, as explained in section 3.1, the y-coordinate of the CMC joint in the optimal configuration is equal to 7.5 cm. The CMC z and x-coordinates provided by the optimization algorithm, are ($z = 5.5$ cm, $y = 6.02$ cm).

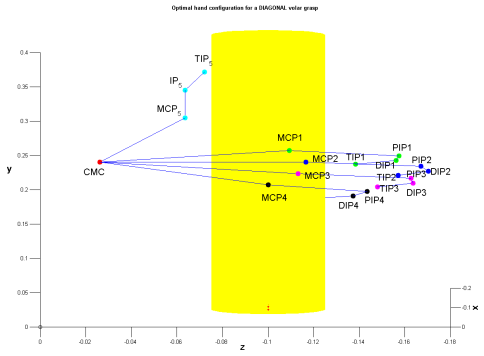

Fig. 8 Plot of the optimal hand configuration, given by the preshaping algorithm, during a diagonal volar grasp.

To reach the optimal final configuration, the hand TIP is controlled in order to describe a spiral trajectory. In the starting configuration of the trajectory planning, the hand is close to the object with the MCP joints in the optimal position given by the optimization algorithm and is open with the fingers parallel to the x-axis of the reference frame. Therefore, the TIP x-coordinates given in input to the trajectory planner, are given by the optimal MCP x-coordinates supplied by the optimization algorithm, plus the length of the links from the MCP joints to the corresponding TIP (obtained from Tab. 4).

The spiral starting radius is given by the sum of the MCP-TIP links of the fingers:

$$r_{init} = a_1 + a_2 + a_3 \tag{9}$$

while the starting angle θ is 90^o. The final radius is given by the distance between the MCP and TIP joints when the TIP joint is in the optimal final position given by

$$r_{final} = \sqrt{(x_{TIP} - x_{MCP})^2 + (y_{TIP} - y_{MCP})^2 + z_{TIP} - z_{MCP})^2} \tag{10}$$

By using the values of the joint inclination angles in the final position, obtained by inverse kinematics, the final value of the angle θ is computed. Figure 9 shows the results obtained in simulation when (8) is applied to a reference position for each finger.

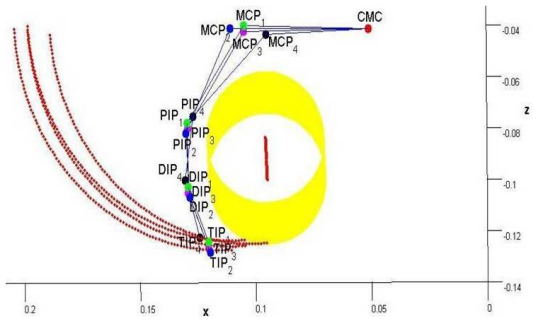

Fig. 9 Red lines show the logarithmic spiral trajectory followed by TIPs when attempting to grasp the object. The y-coordinate of the logarithmic spiral starting points are the same of the corresponding MCP joints.

5 Conclusions

An approach for finding the optimal configuration and finger trajectory of a virtual robotic hand when grasping an object with a diagonal volar grasp has been proposed. The approach is based on the hand kinematic analysis and improves the approaches presented in the literature with the introduction of the thumb behavior. Focussing on the kinematic features related to preshaping has allowed us to finding the optimal preshaping configuration, implementing an algorithm with a reduced computational cost. The algorithm developed for finding the optimal hand configuration is grounded on studies on human grasping carried out with the use of the CyberGlove motion analysis data glove. Performance of the grasp optimization algorithm and of the finger trajectory planning have been tested on a virtual anthropomorphic robotic hand. The simulation results have demonstrated the feasibility of the approach, which seems to enable a human like type of grasping, thus encouraging the experimental validation on a real robotic hand. From a first analysis of the grasping action, it seems possible to make the assumption to extend the approach, valid for the four fingers during a diagonal volar grasp, to the transverse volar grasp (the power grasp where the thumb is abducted). Further work will concern the demonstration of the validity of our assumption by computing some parameters such as finger curvature rays and abduction angles.

Despite the promising results, the joint positions obtained with the CyberGlove do not seem accurate enough to reliably reconstruct the human hand behavior and enable the control of a dexterous robot hand, mainly because of the low acquisition frequency. Therefore, future work will be devoted to (i) carry out experiments with a different motion analysis system, such as stereophotogrammetric systems, with higher performance and data reliability; (ii) apply the algorithm to a real grasping scenario; (iii) extend the approach to transverse volar grasp.

Acknowledgements
This work was supported in part by the national project PRIN/OPENHAND (CUP B81J10000050008) and in part by the European project DEXMART.

References

1. M. Santello, M. Flanders, J.F. Soechting, "Postural hand synergies for tool use", *Journal of Neuroscience*, vol. 18, no. 23, pp. 105–115, 1998.
2. M. Jeannerod, M.A. Arbib, G. Rizzolatti, H. Sakata, "Grasping objects: The cortical mechanisms of visuomotor transformation", *Trends in Neurosciences*, vol. 18, pp. 314–320, 1995.
3. M. Santello, J. Soechting, "Gradual molding of the hand to object contours", *Journal of Neurophysiology*, vol. 79, no. 3, pp. 1307–1320, 1998.
4. G. Schlesinger, "Der mechanische aufbau der kunstlichen glieder", *Ersatzglieder und Arbeitshilfen*, 1919.
5. I.M. Bullock, A.M. Dollar,"Classifying human manipulation behavior", *IEEE International Conference on Rehabilitation Robotics*, pp. 532–537, 2011.
6. D.M. Lyons, "A simple set of grasps for a dextrous hand", *IEEE International Conference on Robotics and Automation*, pp. 588–593, 1985.
7. T. Feix, R. Pawlik, H. Schmiedmayer, J. Romero, D. Kragic, "A comprehensive grasp taxonomy", *Robotics, Science and Systems: Workshop on Understanding the Human Hand for Advancing Robotic Manipulation*, 2009.
8. N. Kamakura, M. Matsuo, H. Ishii, F. Mitsuboshi, Y. Miura, "Patterns of static prehension in normal hands", *American Journal of Occupational Therapy*, vol. 4, no. 7, pp. 437–445, 1980.
9. J.R. Napier, "The prehensile movements of the human hand", *Journal of Bone & Joint Surgery*, vol. 38-B, no. 4, pp. 902–913, 1956.
10. M. Cutkosky, "On grasp choice, grasp models and the design of hands for manufacturing tasks", *IEEE Transactions on Robotics and Automation*, vol. 5, no. 3, pp. 269–279, 1989.
11. Y.Y. Huang, K.H. Low, H.B. Lim, "Initial analysis of EMG signals of hand functions associated to rehabilitation tasks", *IEEE Conference on Robotics and Biomimetics*, pp. 530–535, 2009.
12. B. Buchholz, T. Armstrong, "A kinematic model of the human hand to evaluate its prehensile capabilities", *Journal of Biomechanics*, vol. 25, no. 2, pp. 149–162, 1992.
13. W. Lee, X. Zhang, "Development and evaluation of an optimization-based model for power-grip posture prediction", *Journal of Biomechanics*, vol. 38, no. 8, pp. 1591–1597, 2005.
14. Z. Li, S. Sastry, "Task oriented optimal grasping by multifingered robot hands", *IEEE Journal of Robotics and Automation*, vol. 4, no. 1, pp. 389–394, 1987.
15. A. Bicchi, V. Kumar, "Robotic grasping and contact: a review". *IEEE Conference on Robotics and Automation*, pp. 348–353, 2000.
16. L. Zollo, S. Roccella, E. Guglielmelli, M.C. Carrozza, P. Dario, "Biomechatronic design and control of an anthropomorphic artificial hand for prosthetics and robotic applications", *IEEE/ASME Transactions on Mechatronics*, vol. 12 no. 4, pp. 418–429, 2007.

17. T. Flash, N. Hogan, "The coordination of arm movements: An experimentally confirmed mathematical model", *Journal of Neurophysiology*, vol. 5, no. 7, pp. 1688–1703, 1985.
18. J. Friedman, T. Flash, "Trajectory of the index finger during grasping", *Experimental Brain Research*, vol. 196, no. 4, pp. 497–509, 2009.
19. D.G. Kamper, E.G. Cruz, M.P. Siegel, "Stereotypical fingertip trajectories during grasp", *Journal of Neurophysiology*, vol. 90, no. 6, pp. 3702–3710, 2003.
20. C.L. Taylor, R.J. Schwarz, "The anatomy and mechanics of the human hand", *Artificial Limbs*, vol. 2, no. 2, pp. 22–35, 1955.
21. D.J. Guirintano, A. Hollister, W. Buford, D. Thompson, L. Myers, "A virtual five-link model of the thumb", *Medical Engineering in Physics*, vol. 17, pp. 297–303, 1995.
22. L.Y. Chang, Y. Matsuoka, "A kinematic thumb model for the ACT hand", *2006 IEEE International Conference on Robotics and Automation*, 2006.
23. V.J. Santos, F.J. Valero-Cuevas, "Reported anatomical variability naturally leads to multimodal distributions of Denavit-Hartenberg parameters for the human thumb", *IEEE Transactions on Biomedical Engineering*, vol. 53, no. 2, pp. 155–163, 2006.
24. M. Grebenstein, M. Chalon, G. Herzinger, R. Siegwart, "A method for hand kinematics designers", *1st International Conference on Applied Bionics and Biomechanics*, 2010.
25. P. Cerveri, E. De Momi, N. Lopomo, G. Baud-Bovy, R.M.L. Barros, G. Ferrigno, "Finger kinematic modeling and real-time hand motion estimation", *Annals of Biomedical Engineering*, Vol. 35, no. 11, pp. 1989–2002, 2007.
26. J. Lin, Y. Wu, T.S. Huang, "Modeling the constraints of the human hand motion", *5th Annual Federated Laboratory Symposium*, pp. 121–126, 2001.
27. J. Park, J. Cheong, "Analysis of collective behavior and grasp motion in human hand", *International Conference on Control, Automation and Systems*, pp. 2514–2518, 2010.
28. G. Stillfried, P. van Der Smagt, "Movement model of a human hand based on magnetic resonance imaging (MRI)", *1st International Conference on Applied Bionics and Biomechanics*, 2010.
29. "CyberGlove data glove webpage", *http://www.cyberglovesystems.com*.
30. F. Cordella, L. Zollo, E. Guglielmelli, B. Siciliano, "A bio-inspired strategy for optimal grasp of an anthropomorphic robotic hand", *ViRtual environments and prototyping for huMAN health and safety, Special Track of 9th International Conference IDMME – Virtual Concept*, 2010.
31. J. Lukos, C. Ansuini, M. Santello, "Choice of contact points during multidigit grasping: effect of predictability of object center of mass location", *Journal of Neuroscience*, vol. 27, no. 14, pp. 3894–3903, 2007.

Figure
Click here to download high resolution image

Figure
Click here to download high resolution image

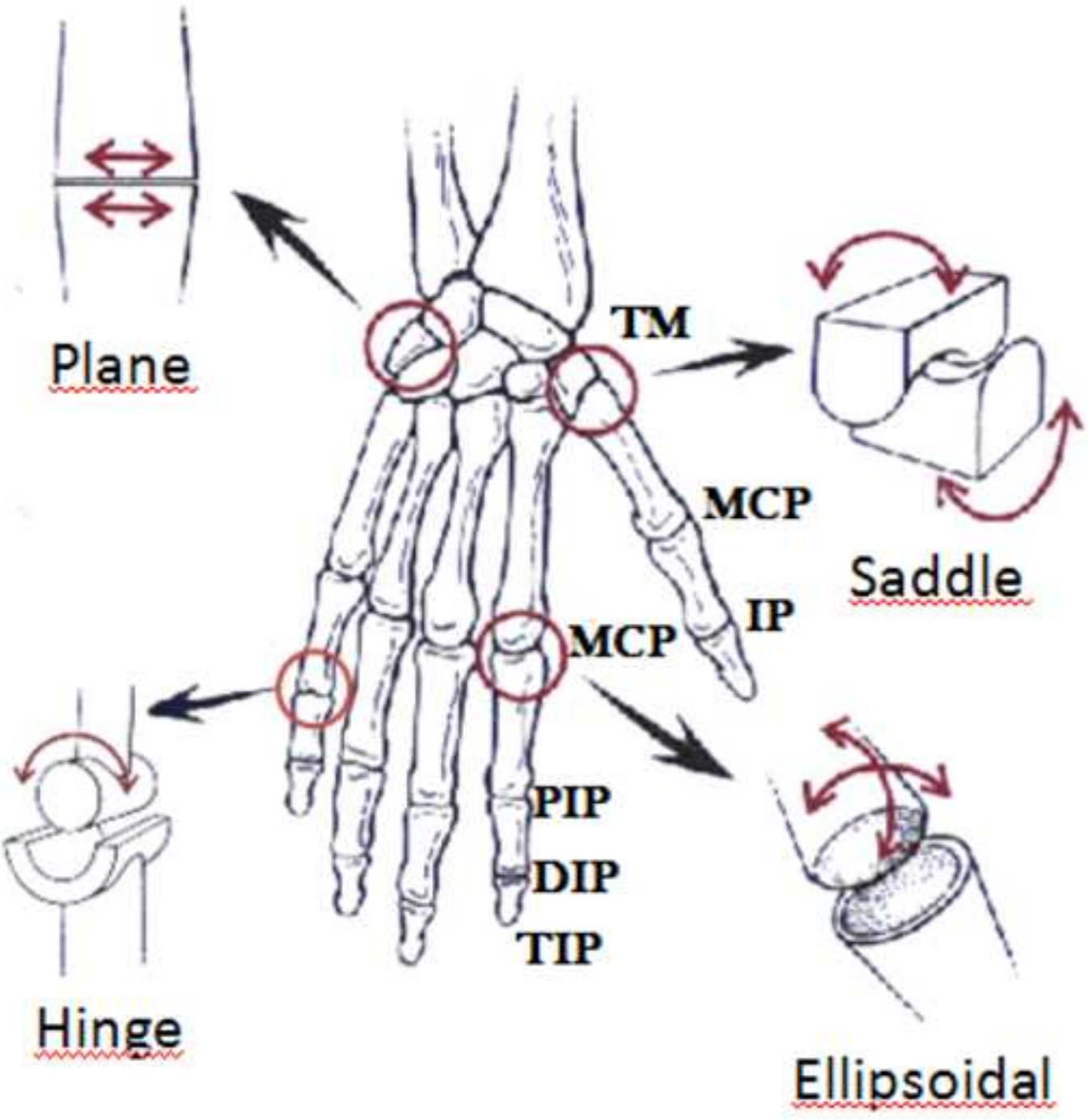

Figure
Click here to download high resolution image

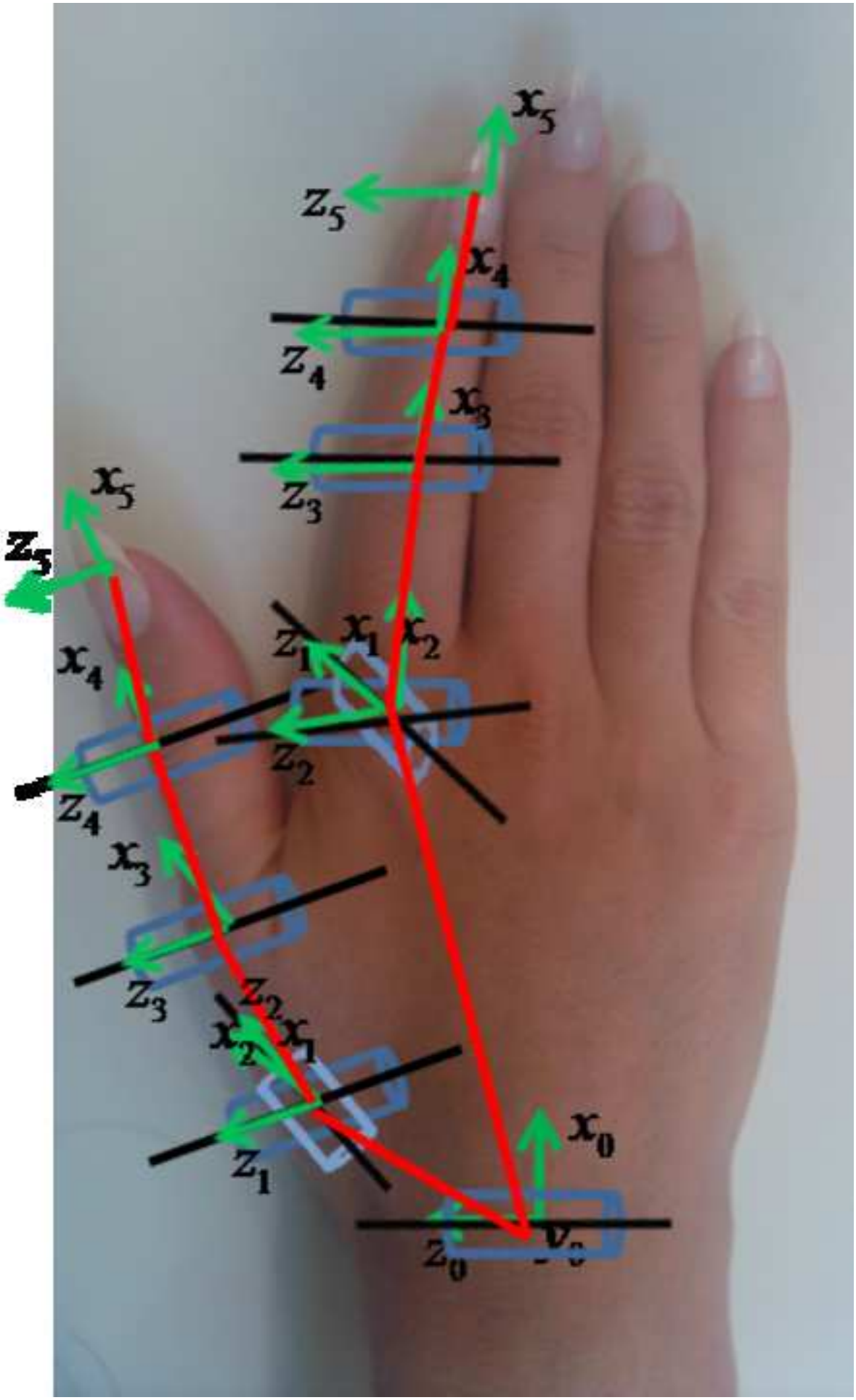

Figure
Click here to download high resolution image

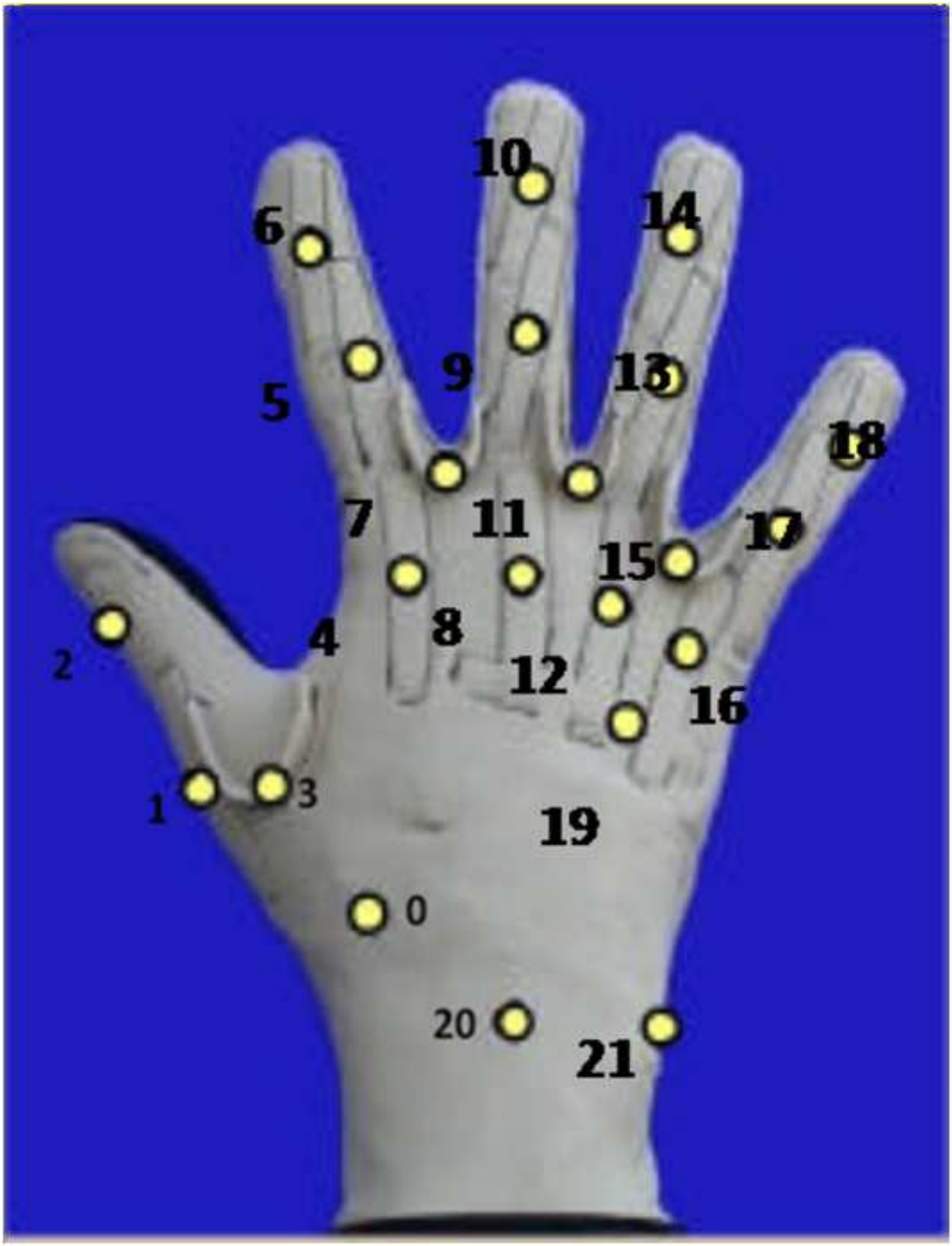

Figure
Click here to download high resolution image

Figure
Click here to download high resolution image

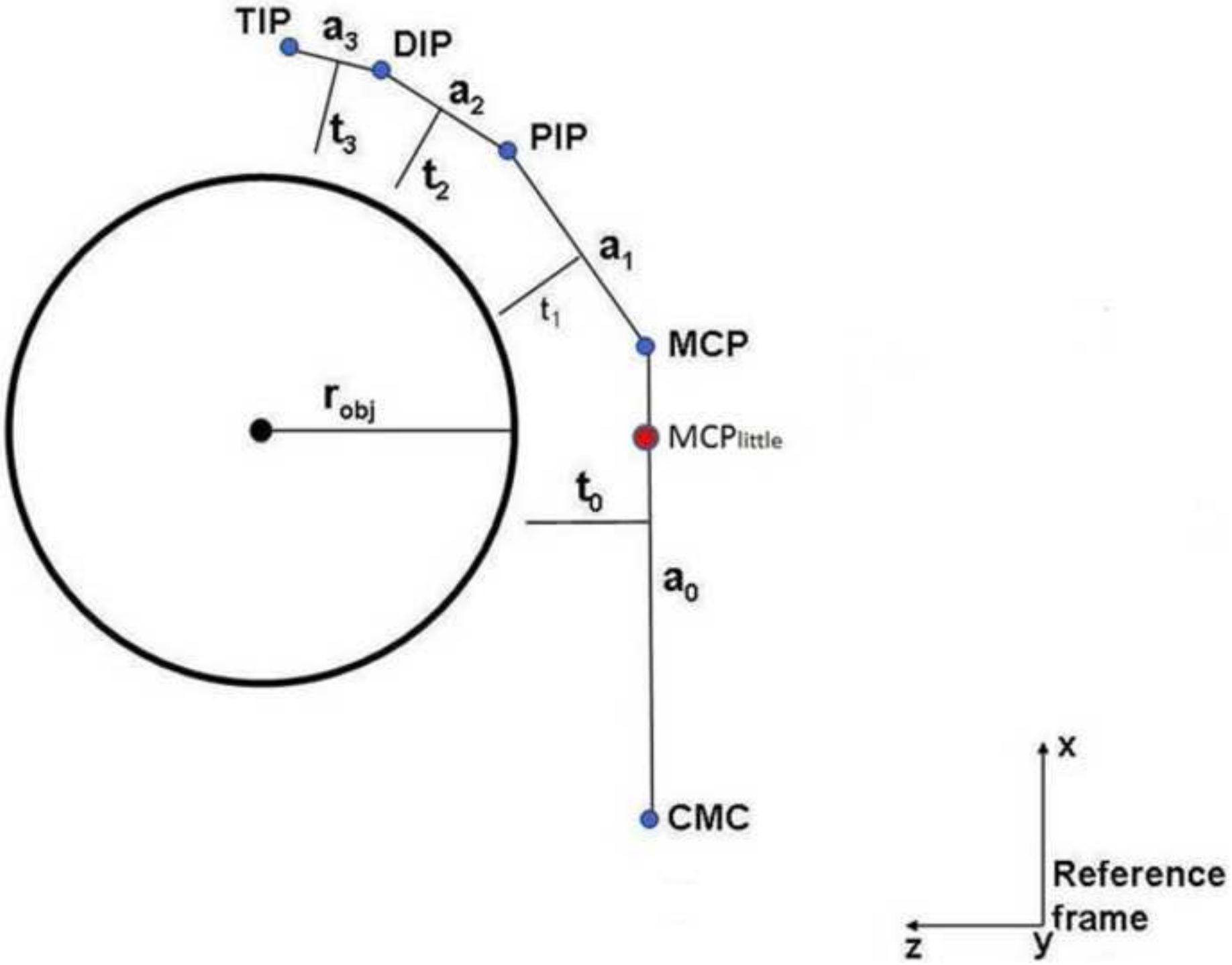

Figure

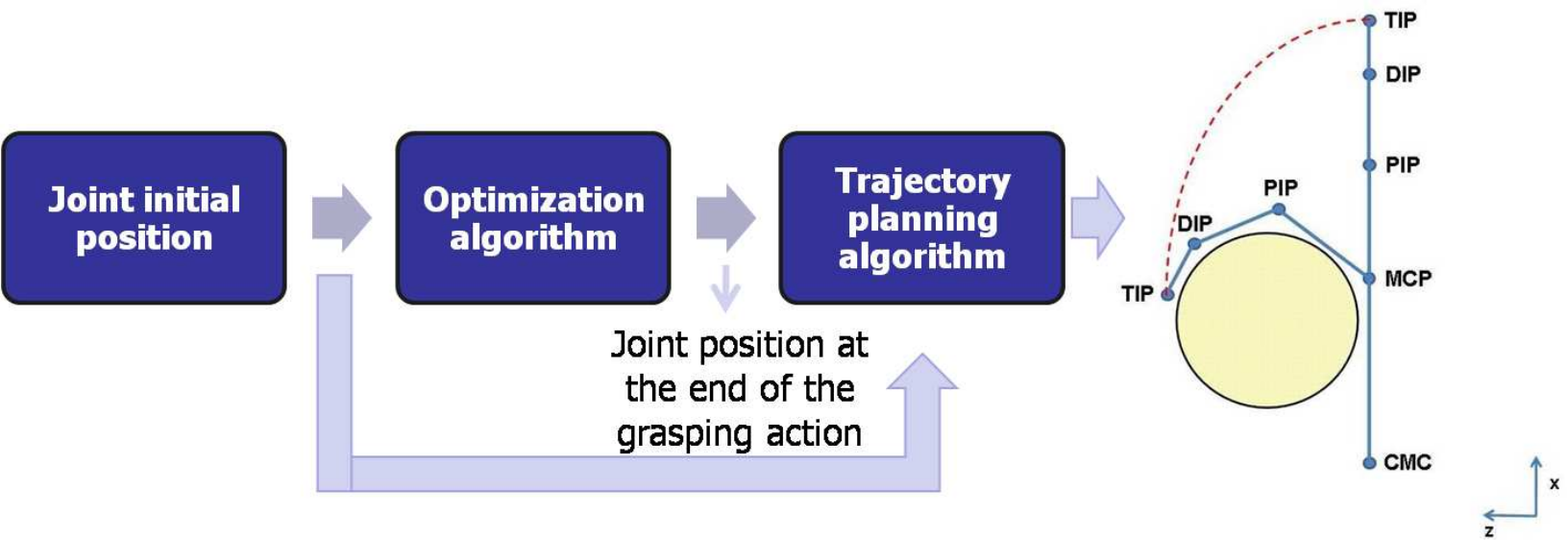
Joint initial position
Optimization algorithm
Trajectory planning algorithm
Joint position at the end of the grasping action
TIP
DIP
PIP
MCP
CMC
x
z

Figure

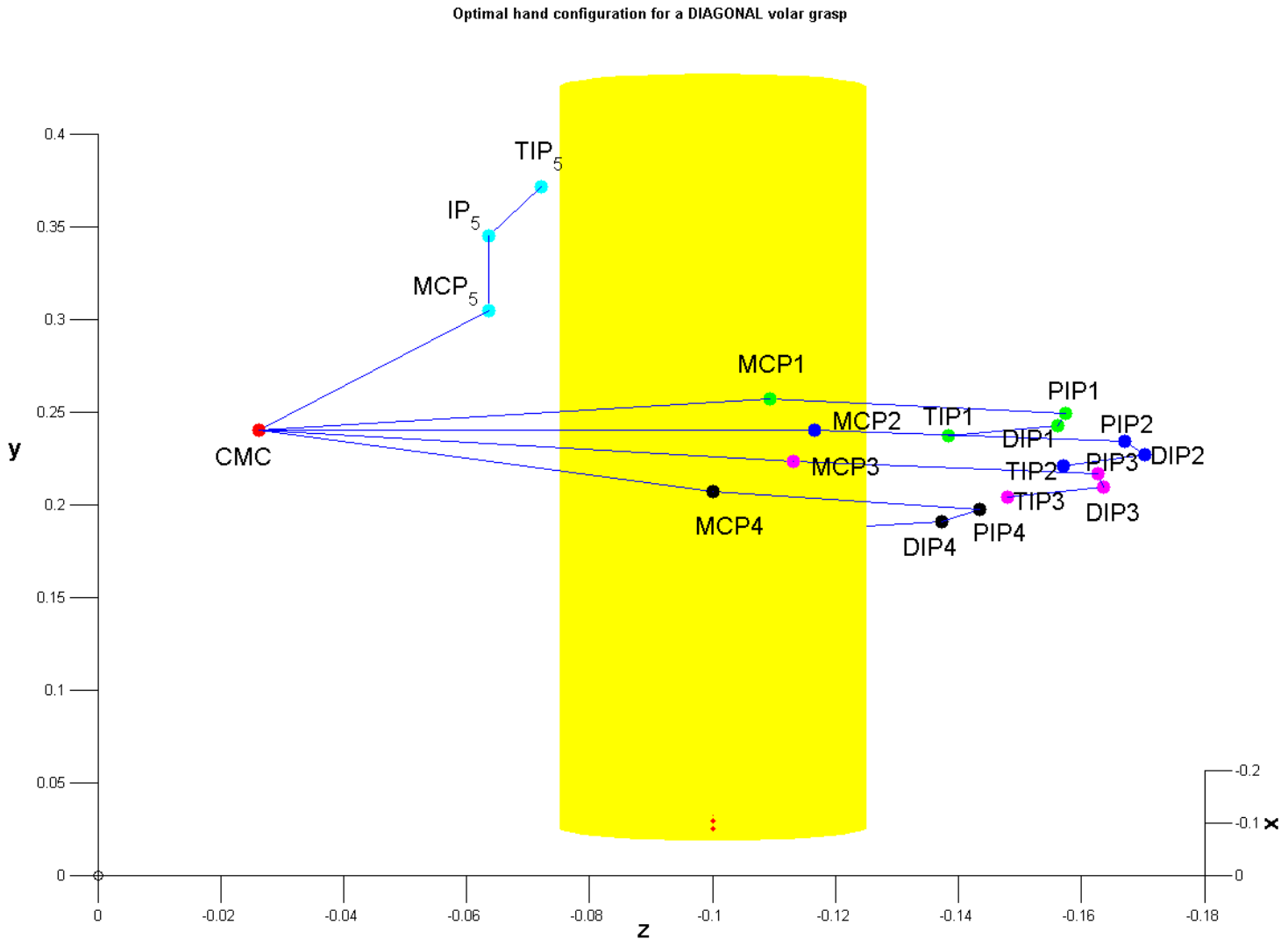
Optimal hand configuration for a DIAGONAL volar grasp
TIP5
IP5
MCP5
MCP1
PIP1
MCP2
TIP1
PIP2
DIP1
CMC
MCP3
TIP2
PIP3
DIP2
TIP3
DIP3
MCP4
PIP4
DIP4
y
z
x
0.4
0.35
0.3
0.25
0.2
0.15
0.1
0.05
0
-0.02
-0.04
-0.06
-0.08
-0.1
-0.12
-0.14
-0.16
-0.18
-0.2
-0.1

Figure

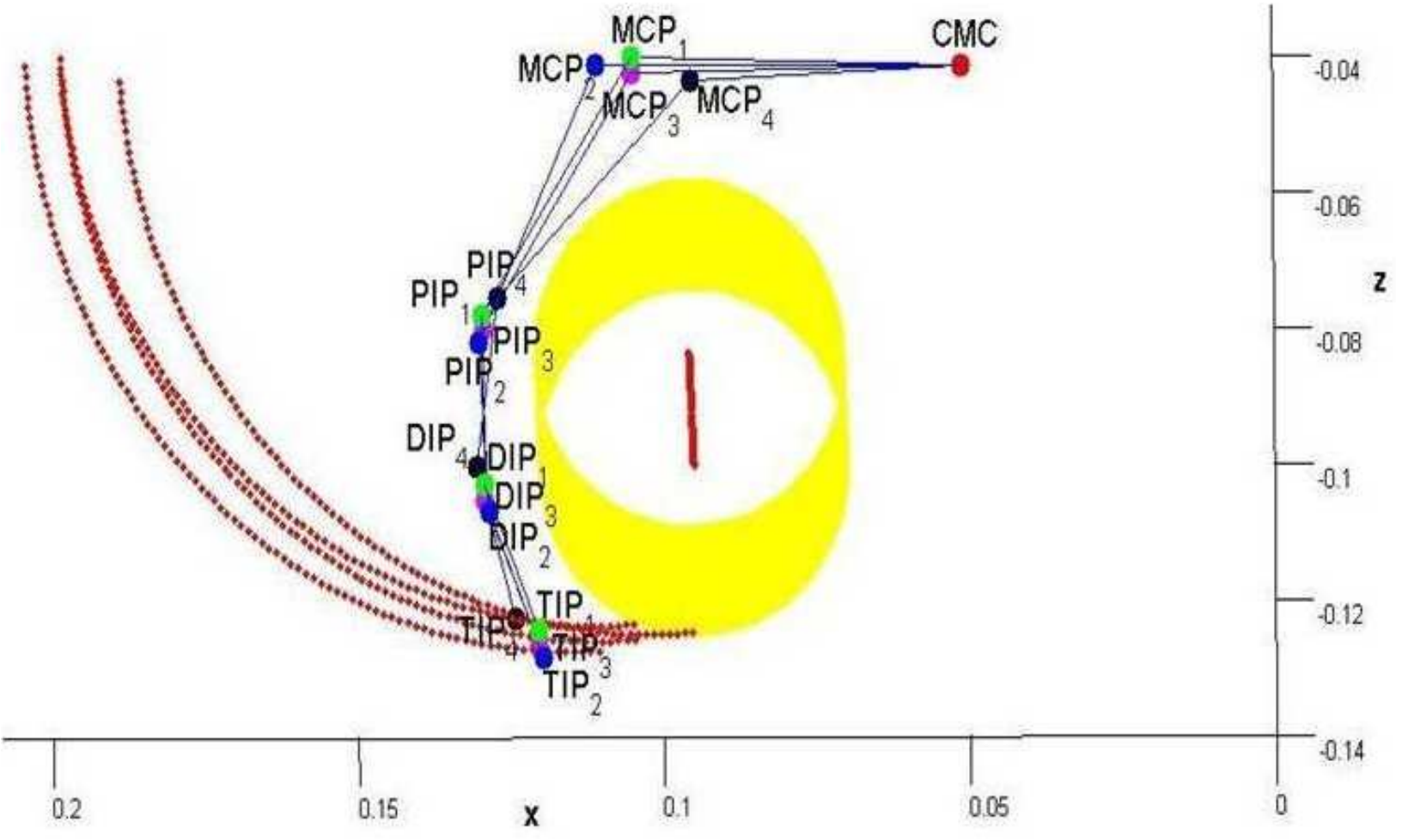
MCP1
CMC
MCP2
MCP3
MCP4
PIP4
PIP1
PIP3
PIP2
DIP4
DIP1
DIP3
DIP2
TIP4
TIP1
TIP3
TIP2
-0.04
-0.06
-0.08
-0.1
-0.12
-0.14
z
0.2
0.15
0.1
0.05
0
x

Table

Table 1 Denavit-Hartenberg parameters of the index finger.

Link #	d	θ	$a\,[m]$	α
1	$d_{1_{\text{index}}}$	θ_1	Mc	$-\frac{\pi}{2}$
2	0	θ_2	0	$\frac{\pi}{2}$
3	0	θ_3	P_{index}	0
4	0	θ_4	M_{index}	0
5	0	θ_5	D_{index}	0

Table

Table 2 Denavit-Hartenberg parameters of the thumb

Link #	d	θ	$a\,[m]$	α
1	$d_{1_{\text{index}}}$	θ_1	Tm	$-\frac{\pi}{2}$
2	$d_{2_{\text{index}}}$	θ_2	0	$\frac{\pi}{2}$
3	0	θ_3	P_{thumb}	0
4	0	θ_4	M_{thumb}	0
5	0	θ_5	D_{thumb}	0

Table

Table 3 Mean and standard deviation of hand opening angle in diagonal volar grasp.

Subject #	Mean	SDV
1	48.63^o	0.77^o
2	49.56^o	1.33^o
3	50.40^o	1.51^o
4	45.87^o	1.45^o
5	45.42^o	1.21^o
6	51.46^o	0.65^o
7	52.57^o	1.18^o
8	50.29^o	0.68^o
9	45.83^o	0.82^o
10	49.75^o	0.93^o

Table

Table 4 Geometric parameters of the simulated hand and object.

Symbol	Link name	value$[m]$
a_0	$CMC - MCP$ link length	0.075
a_1	Proximal link length	0.045
a_2	Medial link length	0.025
a_3	Distal link length	0.023
t_0	Palm thickness	0.025
t_1	Proximal link thickness	0.010
t_2	Medial link thickness	0.0075
t_3	Distal link thickness	0.0025
r_{obj}	Cylindrical object radius	0.0255

Supplementary Material

Click here to download Supplementary Material: A bio-inspired grasp optimization algorithm_blinded.tex

Supplementary Material

Click here to download Supplementary Material: subfigure.sty